Plant-wide control design based on steady-state combined indexes

David Zumoffen[a,1,*]

[a]*Process System Engineering Group (PSEG). French-Argentine International Center for Information and Systems Sciences (CIFASIS-CONICET-UNR-AMU), 27 de Febrero 210 bis, (S2000EZP) Rosario, Argentina. TE: +54-341-4237248 int. 332, Fax: +54-341-4821772*

Abstract

This work proposes an alternative methodology for designing multi-loop control structures based on steady-state indexes and multi-objective combinatorial optimization problems. Indeed, the simultaneous selection of the controlled variables, manipulated variables, input-output pairing, and controller size and interaction degree is performed by using a combined index which relies on the sum of square deviations and the net load evaluation assessments in conjunction. This unified approach minimizes both the dynamic simulation burden and the heuristic knowledge requirements for deciding about the final optimal control structure. Further, this methodology allows incorporating structural modifications of the optimization problem context (degrees of freedom). The case study selected is the well-known Tennessee Eastman process and a set of simulations are given to compare this approach with early works.

Keywords: Multi-loop Control Structure, Plantwide Control Design, Combined Index, Structural Process Faults

1. Introduction

1.1. Process control

Industrial processes generally involve several operating units interconnected via some specific layout, which is designed for fulfilling some requirements related to product quality, product rate, and profits. The major drawbacks limiting any kind of analysis on these processes are their respective size and complexity. The size of the process is related obviously with the number of units and variables involved. The complexity characteristic is tied to the high energy and mass integration of the plant. The current tendency in processes design is to increase this complexity for reducing the operating cost and maximizing the profits [1, 2]. Furthermore, for avoiding the adverse effects of disturbances and ensuring safety, robustness, stability, product qualities, and profits, these industrial processes need to be controlled in some extent. Generally, multi-loop (several single-input/single-output loops) control structures are used to this end.

*Corresponding author
Email address: zumoffen@cifasis-conicet.gov.ar (David Zumoffen)
[1]Also with Universidad Tecnológica Nacional – FRRo, Zeballos 1341, (S2000BQA) Rosario, Argentina

It is worth mentioning that any control policy requires several decisions before it will be considered as a potential and feasible control structure. In fact, typical decisions involve the proper selection of the following constitutive parts: the controlled variables (CVs), the manipulated variables (MVs), the input-output pairing between these sets, and various characteristics associated with the controller itself, such as the interaction degree (diagonal, sparse, full), policy (decentralized or centralized), tuning, and technology (classical or advanced). Plant-wide control (PWC) is a very important area to address the previously mentioned decisions. The overall performance as well as the investment/operating cost can be seriously affected if the PWC problem is not solved properly [3, 4]. The complexity of the PWC problem increases with the process dimensions. In some cases, a heuristic and exhaustive treatment (the classical approach) is not possible. In this context it is very useful some systematic and generalized (holistic) methodology to overcome these drawbacks. Anyway, the latter solution requires the integration of several knowledge bases with different insights which shows the complexity of an unified (all in one) methodology [3]. These large and complex problems are some examples of new trends which need to be addressed in the process systems engineering (PSE) area [5].

1.2. Plant-wide control overview

An overview on the PWC approaches existing in literature clearly identifies three point of views: 1- methods based on purely heuristic/engineering judgment [6, 7], 2- strategies based on mathematical/systems theory [8], and 3- approaches based on integration/hybrid [2]. All these methodologies suggest different ways to design decentralized PWC structures addressing all the major process control implications [9]. The heuristic methods, which are systematic in nature, were tested extensively in many case studies. However, for large-scale processes several ad-hoc considerations are required to progressively reduce the dimension of the PWC problem until reaching handle dimensions. This drawback generally produces suboptimal designs from the operating as well as investment cost perspectives. On the other hand, the advent of computing power favored an intense research and development in the mathematical/systems theory as well as hybrid based methods. Indeed, the last three decades, this application field has generated countless proposals with varied themes including: stability/controllability/robust assessments [10–12], input-output pairing problems [13–15], operating cost and self-optimizing control [3, 16, 17], deviations-based indexes [18, 19], exergy eco-efficiency factor/thermodynamic concepts [2, 20], combination of these into a multi-objective criteria [3, 4, 19], and integration between heuristics and steady-state/dynamic simulations [2, 9]. All these mathematical approaches are based on process models, whether they are dynamic or steady-state, linear or nonlinear, whereby these design depend on the accuracy and availability of these simplifications. It is important to note that, for large-scale industrial processes, it is very difficult to obtain a control-oriented process model. Generally, it is more common to deal with steady-state models which come from the process design and synthesis stages.

1.3. Comments on the case study

The case study considered in this paper is the well-known Tennessee Eastman Process (TEP), which was proposed by Downs and Vogel [21] as a multivariable nonlinear benchmark plant for the process control community. Although the original TEP version was modeled in Fortran, the current work is based on the Matlab dynamic simulator generated by compiling the source code which is available from the Prof. Ricker's web page [22].This precursory work summarizes the potential working modes (six) and the general control scenarios (four set points to be tracked and twenty disturbances to be rejected) to properly operate the process. Specific details about this plant are given in the case study section. While Downs and Vogel [21] suggest (from a qualitative comparison point of view) only consider one specific mode (base case), four set points (production rate and mix, reactor pressure, and B composition in purge), and five particular disturbances (IDV1, IDV4, IDV8, IDV12, and IDV13), other authors have been proposed and developed the most variated PWC designs under the most variated scenarios and methodologies. In this context an exhaustive comparison becomes complex, incomplete or impossible for some approaches. Indeed, the most relevant applications for designing multiloop control structures are summarized in the following. Within the heuristic-based PWC design can be found works using steady-state screening tools [23]; approaches based on the tired method and process insights [24, 25], and designs based on the nine steps approach [26]. Some mathematical approaches also appear based on thermodynamic theory to define the most dominant variables [27]; steady-state optimization for analyzing operating costs and variable vinculations [28]; and methodologies based on the self-optimizing control strategy to guarantee the optimal operation [29]. Finally, some designs are focused on integrated tools such as mathematics, heuristics, and simulations (steady-state or dynamic) [9]. It is worth mentioning that all the above approaches (and many others) give stable PWC structures with similar dynamic performances, where most of them are implemented based on decentralized feedback control approaches and then improved by adding some kind of feedforward, override, ratio, and selective controllers. All these integrated and complex designs arise from the need to address properly the changing and strongly nonlinear behavior of the process when the latter is forced to operate in several modes and optimal working points.

1.4. Existing drawbacks and contribution of the work

Four common drawbacks can be identified from above discussed approaches: 1- heuristic-based method requires an ad-hoc reduction of the problem size for large-scale process, generating suboptimal designs from simplicity, investment/operating costs, and/or robustness characteristics [30], 2- most of mentioned design tools use all the available degrees of freedom (DOF) which leads unnecessarily to overdimensioned designs, i.e. the simplest structure is preferred [26], 3- accurate dynamic models are infrequent for real cases, the common scenario is confined to steady-state models either linear or nonlinear, and 4- most of commented

approaches are focused on getting decentralized (diagonal) multivariable feedback control structures as a base control policy.

In this work, an alternative PWC design methodology is proposed to overcome the above mentioned drawbacks. The overall approach is based on a single multi-objective combinatorial optimization problem with steady-state functional costs. This mathematical representation allows considering the original size of the problem without any ad-hoc reduction, furthermore any a priori heuristic consideration may be included properly via weighting matrices. The unified programing suggested here consists of two steady-state contributions called the sum of square deviations (SSD) and the net load evaluation (NLE) indexes, which have strong connection with the controllability/performance properties of the current PWC [18, 31]. This new optimization problem allows to define the CVs, MVs, controller order/size, the input-output pairing, and the controller interaction, simultaneously. Hence, several different DOF may be evaluated and no dynamic models are needed in this design stage. This feature generalizes and systematizes the overall PWC design procedure focusing the search to simple feedback control structures. Moreover, the NLE component gives relevant information related to the controller interaction and how this structure affects the closed-loop performance [31]. Thus, if required, integrated multi-loop control policies (feedback and feedforward) can be designed eventually as base structure. This new unified strategy is particularly interesting because it is well suited to handle any potential modification of the PWC problem context, i.e. DOF changes. A particular DOF situation may change due to multiple expected and unexpected factors [32]. In the present work, an alternative application is proposed when the DOF change due to structural process faults such as sensor and/or actuator malfunctions. Moreover, security/stability control loops are suggested, for some particular abnormal events, directly related to the override/selective controllers concepts from industrial practice [33, 39].

It is worth mentioning that the proposed methodology for PWC design is mainly focused to control structure design and evaluation from the conceptual engineering point of view. It allows to select valid control policies by using limited information (steady-state) and analyze potential DOF modifications. The application suggested here, related to structural process fault, is not aimed to be an active fault-tolerant control approach and/or an on-line redesign methodology. The main real application is to analyze (off line) potential PWC structures, how the performance of these policies are affected by eventual structural process faults, and if hardware redundancy could be useful in some extent. Thus, relevant information can be obtained, for example, for the process synthesis and design stage.

The case study selected here is the well-known TEP problem, briefly mentioned in previous paragraphs. Although the overall PWC design is based on steady-state information only, all the suggested control policies are tested dynamically by using the non linear simulator in the MatLab context. Due to the diverse range of existing PWC proposals on this process, the main comparison tasks are focused on structural resemblances and hardware requirements among them. All the optimization problems presented in this

work rely on multi-objective combinatorial representations and were efficiently solved via stochastic global search such as genetic algorithms (GA). While the GA-based optimizations suffer from uncertainty related to the global optimum, the main reason to use these algorithms lies in the ease of both representation as well as implementation. This fact is very important from the engineering point of view. Particularly, the open code given by Chipperfield et al. [34] is used here. It is important to note that the same combinatorial problem may be solved by deterministic mixed-integer optimization based formulations, for example in the GAMS environment. Indeed, the integration between process synthesis and control, in the GAMS environment, is currently under development by the author and co-workers. In future works a complete representation will be given in a deterministic optimization context.

2. Analyzing PWC scenarios

In the following sections, alternative methodologies for PWC design are presented. In all cases, the approaches are based on analyzing several control structures by integrating the SSD and NLE concepts and suggesting a simultaneous CVs and MVs selection according to the DOF available in the process, i.e. plant-wide control scenarios. Although the strategies are not holistic approaches, they have some systematic and generalization degree by minimizing the heuristic considerations.

The potential multivariable control alternatives depend on: 1- the process (the number of potential outputs m and manipulated variables n) and 2- the control requisites (the number of control loops needed $q = q_o + q_a$). Where q_o is the number of output variables which must be controlled *"indefectibly"* (process engineering requirements: production rate, product quality, etc.) and q_a is the number of additional output variables which *"could/should"* be controlled in order to complete the multivariable controller configuration.

Although q_a may be null, generally it affects the order/size of the final controller to be implemented. Indeed, a common practice in most of the existing PWC design methods is to select q_a by considering all the potential DOF available, i.e. $q_a = n - q_o$ for the $m > n$ case. In this section a complete evaluation of several PWC structures is proposed by analyzing all the potential range $0 \leq q_a \leq \min(m, n) - q_o$. In this context, the potential plant-wide control alternatives are divided into four cases:

Case I: MVs Selection ($m < n$, $q = m$). There are more MVs than CVs and all the outputs need to be controlled.

Case II: Simultaneous CVs and MVs selection ($m \lesseqgtr n$). Several process topologies need to be considered where $q < \min(m, n)$, i.e. all the potential DOF are not required to be used.

Case III: CVs selection ($m > n$, $q = n$). There are more CVs than MVs and all the available inputs are used in the control structure, i.e. all DOF used.

Case IV: There are no alternatives ($m = n = q$). The next step is the input-output pairing selection via relative gain array (RGA) for example.

Each scenario requires a particular approach for solving the original PWC problem. Furthermore, the existing control structure design tools are based only on cases I, II, or IV individually. In contrast, Zumoffen [19] suggests a PWC design approach by addressing the oversizing analysis for all the cases simultaneously. This strategy is called here the classical EMSD approach.

3. Classical and modified EMSD methodologies

This section summarizes the main ideas behind both the classical and the modified EMSD methodologies. Initially, the classical EMSD approach suggested in Zumoffen [19] is presented briefly only for contextualizing the improvements proposed further in this work.

Let us assume a stable (or already stabilized) plant with the transfer functions matrix (TFM) representation (in Laplace domain) given in Eq. (1),

$$\mathbf{y}(s) = \begin{bmatrix} \mathbf{y}_s(s) \\ \mathbf{y}_r(s) \end{bmatrix} = \begin{bmatrix} \mathbf{G}_s(s) & \mathbf{G}_s^*(s) \\ \mathbf{G}_r(s) & \mathbf{G}_r^*(s) \end{bmatrix} \begin{bmatrix} \mathbf{u}_s(s) \\ \mathbf{u}_r(s) \end{bmatrix} + \begin{bmatrix} \mathbf{D}_s(s) \\ \mathbf{D}_r(s) \end{bmatrix} \mathbf{d}(s) \tag{1}$$

where the number of potential CVs, available MVs, and disturbance variables (DVs) are m, n, and p, respectively.

The subsystems and signals involved in Eq. (1) have the following description:

- $\mathbf{G}_s(s)$ is the square $(q \times q)$ subprocess to be controlled,
- $\mathbf{u}_s(s)$ are the $(q \times 1)$ selected MVs subset for controlling the $(q \times 1)$ output variables subset $\mathbf{y}_s(s)$,
- $\mathbf{u}_r(s)$ are the $((n-q) \times 1)$ remaining input variables which are not used for control purposes and $\mathbf{y}_r(s)$ are the $((m-q) \times 1)$ uncontrolled variables (UVs),
- $\mathbf{G}_s^*(s)$, $\mathbf{G}_r(s)$, $\mathbf{G}_r^*(s)$, are remaining matrices with dimension $(q \times (n-q))$, $((m-q) \times q)$, $((m-q) \times (n-q))$,
- $\mathbf{D}_s(s)$ $(q \times p)$ and $\mathbf{D}_r(s)$ $((m-q) \times p)$ are the disturbance matrix partitioning which affect the CVs and UVs, respectively,

where $q \leq \min(m, n)$ represents the number of variables which should be controlled, i.e. the control requisites. On the other hand, $\mathbf{u}(s) = [\mathbf{u}_s(s)\, \mathbf{u}_r(s)]^T$ and $\mathbf{d}(s)$ represent the input and disturbance vectors respectively.

Let us consider that the subprocess $\mathbf{G}_s(s)$ is controlled via some structure with integral action. In fact, the internal model control (IMC) approach is considered here, where $\mathbf{G}_c(s) = \tilde{\mathbf{G}}_s^{-1}(s)\mathbf{F}(s)$ is the controller,

$\tilde{\mathbf{G}}_s(s)$ the process model and $\mathbf{F}(s)$ a low-pass TFM. If the inputs $\mathbf{u}_r(s)$ are not used for control purposes, then the following relationships can be stated for the MVs, CVs, and UVs, respectively

$$\begin{aligned}
\mathbf{u}_s(s) &= \mathbf{G}_s^{-1}(s)\mathbf{y}_s(s) - \mathbf{G}_s^{-1}(s)\mathbf{D}_s(s)\mathbf{d}(s) \\
\mathbf{y}_s(s) &= \mathbf{F}(s)\mathbf{y}_s^{sp}(s) + (\mathbf{I} - \mathbf{F}(s))\mathbf{y}_s^{net}(s) \\
\mathbf{y}_r(s) &= \mathbf{G}_r(s)\mathbf{G}_s^{-1}(s)\mathbf{y}_s(s) + \left(\mathbf{D}_r(s) - \mathbf{G}_r(s)\mathbf{G}_s(s)^{-1}\mathbf{D}_s(s)\right)\mathbf{d}(\mathbf{s})
\end{aligned} \tag{2}$$

with $\mathbf{S}_{sp}(s) = \mathbf{G}_r(s)\mathbf{G}_s^{-1}(s)$, $\mathbf{S}_d(s) = \left(\mathbf{D}_r(s) - \mathbf{G}_r(s)\mathbf{G}_s^{-1}(s)\mathbf{D}_s(s)\right)$, and $\mathbf{y}_s^{net}(s) = \mathbf{A}_n(s)\mathbf{y}_s(s) + \mathbf{B}_n(s)\mathbf{d}(s)$ is the so called net load effect (see AppendixA for more details).

For a particular dimension of the subprocess $\mathbf{G}_s(s)$, the corresponding CVs and MVs subsets need to be defined. In this work, the binary decision vectors called $\mathbf{C}^c$ and $\mathbf{C}^m$ parameterize this selection, respectively. On the other hand, a binary decision matrix Γ is also defined for parameterizing the plant-model mismatch via $\tilde{\mathbf{G}}_s(s) = \mathbf{G}_s(s) \otimes \Gamma$, where $\otimes$ represents the Hadamard product (see AppendixA and AppendixB).

Both binary representations are very useful for developing the EMSD method shown in Fig. 1. Basically, this approach is a sequential procedure where combinatorial problems and dynamic simulations are integrated. First, the SSD index is solved for each PWC scenario ($0 \leq q_a \leq \min(m,n) - q_o$) and then all the optimal solutions ($\min(m,n) - q_o + 1$) are simulated for choose the best decentralized control policy. Eventually, the optimal sparse control structure (controller with arbitrary interaction) can be designed based on the previously selected decentralized PWC. Finally, all the multi-loop control structures are simulated for deciding the best one. According to the PWC scenarios analyzed in the previous section, the performance indexes used in each minimization are summarized in Table 1 (see AppendixA). Moreover, the problem dimension is also presented. Henceforth, $\mathbf{A}(\mathbf{C}^c, \mathbf{C}^m)$ and $\mathbf{A}(\Gamma)$ represents a particular selection of rows/columns and entries of the matrix $\mathbf{A}$, respectively.

Remark 1: It is worth mentioning that the SSD and NLE indexes are computed at steady state, where $s = 0$ and $\mathbf{y}_s = \mathbf{y}_s^{sp}$ due to the integral action. The SSD quantifies the deviations produced by set points and disturbance changes in the UVs and/or MVs. This index is directly related to the controllability characteristic of $\mathbf{G}_s(s)$, i.e. if there are potential conflicting direction for control purposes [18, 19]. On the other hand, the NLE measures the deviations produced by the same effects in the $\mathbf{y}_s^{net}(s)$, i.e. how the CVs are affected in the transient by the selected plant-model mismatch [31]. See AppendixA for specific details.

Remark 2: Although the EMSD strategy in Fig. 1 gives a significant reduction of the PWC problem dimension and minimizes several exhaustive evaluations, the final decisions about the control structure is taken based on multiple dynamic simulations. Indeed, it is required to analyze $\min(m,n) - q_o + 1$ decentralized control structures plus one sparse control policy under several scenarios given by the case study.

3.1. Modifications to the EMSD approach: the SSD-NLE combined index

The main idea here is modifying the classical EMSD approach to facilitate the final selection of the multi-loop control structures by minimizing the dynamic simulations burden and the heuristic knowledge requirements (commented previously in remark 2). In this case, a new combined index is proposed based on the SSD and NLE quantifications. Moreover, in this new version the simultaneous selection of MVs, CVs, the number of additional control loops q_a, the input-ouput pairing, and the controller interaction is proposed in a single optimization routine.

In fact, the parametrization variable $\mathbf{C}_i$ suggested in Eq. (3) is used here for contextualizing the overall problem into the GA environment (see AppendixB),

$$\mathbf{C}_i = \left[\mathbf{C}_i^q, \mathbf{C}_i^c, \mathbf{C}_i^m, \mathbf{C}_i^\Gamma, \mathbf{C}^o\right] = \left[\mathbf{C}_i^d, \mathbf{C}^o\right] \tag{3}$$

where $\mathbf{C}_i^d = \left[\mathbf{C}_i^q, \mathbf{C}_i^c, \mathbf{C}_i^m, \mathbf{C}_i^\Gamma\right]$ is de integer/binary decision variable for the GA routine, i represents a particular evaluation/instance (individual from the GA point of view) and $\mathbf{C}^o$ is a fixed variable representing the original control requisites (ad-hoc selection of some CVs). The constitutive vectors have the following dimensions:

$$\mathbf{C}_i^q : (1 \times r) \quad \mathbf{C}_i^c : (1 \times (m - q_o)) \quad \mathbf{C}_i^m : (1 \times n) \quad \mathbf{C}_i^\Gamma : (1 \times (s-1)s) \quad \mathbf{C}^o : (1 \times q_o), \tag{4}$$

where $\mathbf{C}_i^c$ is the additional CVs selection according to the q_a variable, and $\mathbf{C}_i^m$ defines the MVs selected for squaring down the control problem. The variable called $\mathbf{C}_i^q$ defines the number of additional control loops required q_a, either in binary or integer representation. In the binary case, r must be adequate for representing all the q_a integer numbers in the range $0 \leq q_a \leq \min(m,n) - q_o$. Finally, $\mathbf{C}_i^\Gamma$ is a binary vector which represents the off-diagonal elements needed to be included in the parametrization matrix Γ for designing the IMC controller interaction, where $s = \min(m,n)$. The length of the decision variable $\mathbf{C}_i^d$ results $n_c = r + (m - q_o) + n + (s-1)s$. Note that, the IMC controller is given by $\mathbf{G}_c(s) = (\mathbf{G}_s(s) \otimes \Gamma)^{-1}\mathbf{F}(s)$ (see AppendixA).

The sequential EMSD method shown in Fig. 1 can be unified into a single multi-objective combinatorial

problem as:

$$\min_{(\mathbf{C}_i)} \left[\text{SSD}_{\mathbf{y}_r}(\mathbf{C}_i) + \text{NLE}_{\Gamma}(\mathbf{C}_i)\right], \tag{5}$$

$$\text{subject to} \quad q_a = \mathbf{C}_i^q \leq \min(m,n) - q_o, \tag{6}$$

$$||\mathbf{C}_i^c||_1 = q_a, \tag{7}$$

$$||\mathbf{C}_i^m||_1 = q_a + q_o, \tag{8}$$

$$\det(\mathbf{G}_s) \neq 0, \tag{9}$$

$$\mathbf{p}_{op} = \arg\min_{\mathbf{p}_i} \Lambda_n(\mathbf{G}_s(\mathbf{p}_i)), \tag{10}$$

$$\mathbf{C}_i^{\Gamma q_a} = \mathbf{C}_i^{\Gamma}\left(1 : (q_o + q_a - 1)(q_o + q_a)\right), \tag{11}$$

$$\Gamma = \mathbf{I} + f(\mathbf{C}_i^{\Gamma q_a}), \tag{12}$$

$$\tilde{\mathbf{G}}_{s\Gamma} = \mathbf{G}_s \otimes \Gamma, \tag{13}$$

$$\text{Re}\left[\lambda_i\left(\mathbf{G}_s \tilde{\mathbf{G}}_{s\Gamma}^{-1}\right)\right] > 0,\ i = 1, \ldots, q_a + q_o. \tag{14}$$

It is important to note that the evaluation of $\text{SSD}_{\mathbf{y}_r}$ as well as NLE_{Γ} require the matrices $\mathbf{G_s}$, $\mathbf{G_r}$, $\mathbf{D_s}$, and $\mathbf{D_r}$ which are functions of the parametrization variable $\mathbf{C}_i = \left[\mathbf{C}_i^q, \mathbf{C}_i^c, \mathbf{C}^o, \mathbf{C}_i^m, \mathbf{C}_i^{\Gamma}\right]$ and the main process matrices $\mathbf{G}$ and $\mathbf{D}$. The constraint in Eq. (6) guarantees that the selected q_a belongs to the feasible PWC alternatives/scenarios. In this case an integer representation for q_a was selected. Constraints in Eqs. (7)-(8) ensure that the number of selected CVs and MVs, in $\mathbf{C}_i^c$ and $\mathbf{C}_i^m$, are made properly by considering the suggested q_a number. This conditions allow to square-down the overall PWC problem. In the IMC context, is important guaranteeing the model inversion at steady-state, so constraint in Eq. (9) ensures this characteristic. For computing NLE_{Γ}, the matrices $\mathbf{G_s}$ and $\tilde{\mathbf{G}}_{s\Gamma} = \mathbf{G_s} \otimes \Gamma$ are required to be diagonally paired. Hence, some systematic methodology is needed to perform this task into the optimization routine, i.e. constraint Eq.(10). Section 3.1.1 summarizes some details about the proposed automatic input-output pairing subproblem based on the RGA-number. Equality in Eq.(11) allows selecting the first $(q_o + q_a - 1)(q_o + q_a)$ entries from the vector $\mathbf{C}_i^{\Gamma}$ to be used as decision variables. It is clear that the size of $\mathbf{C}_i^{\Gamma q_a}$ depends on the current q_a selected. Note that Eq.(12) defines the current controller interaction matrix Γ used. In fact, $f(\mathbf{C}_i^{\Gamma q_a})$ is a function which builds a $(q_o+q_a)\times(q_o+q_a)$ binary matrix with null entries in the main diagonal and the elements suggested by $\mathbf{C}_i^{\Gamma q_a}$ in the off-diagonal components. It is worth mentioning that if only decentralized PWC structures are preferred (not sparse or full), then the vector $\mathbf{C}_i^{\Gamma}$ can be fixed to zero or eventually removed. The last constraint in Eq. (14) is the stability/robustness criterion developed by Garcia and Morari [35] for multivariable control structures based on IMC theory, where Re[$\cdot$] is the real part function, $\lambda_i(\cdot)$ is the i-th eigenvalue, and $\tilde{\mathbf{G}}_{s\Gamma}$ the model parametrization/selection.

The main steps of the suggested SSD-NLE index based approach are shown in Fig 2. The procedure begins with the initialization stage where the process steady-state gains, their corresponding sizes, and the

original control requisites are given. The next step is testing the current PWC scenario according to the classification given in section 2. The so called Case IV means that CVs and MVs are not required to be defined. Therefore, the left branch in the block diagram is activated and it enables the optimal input-ouput pairing evaluation via the subproblem in Eq.(10)/Section 3.1.1. With a decentralized control structure already defined, the controller interaction could be investigated if the main optimization problem Eq.(5) to Eq.(14) is solved by using only the constraints Eq.(11) to Eq.(14), the NLE index from Table 1 as the main functional cost, and $n_c = (q-1)q$. On the other hand, for Cases I, II, and III the branch to be followed is the central path of the block diagram. Indeed, the next step is selecting the controller structure desired: 1- without interaction (diagonal), where $\mathbf{C}_i^{\Gamma}$ is not required to be computed in the main problem ($s = 0$), or 2- with interaction (full/sparse), where $\mathbf{C}_i^{\Gamma}$ is needed according to Eq. (4) ($s = \min(m, n)$). This stage is followed by the proper setting of the GA routine: size of the initial population, number of generations, amount of selected individuals for matting, crossover and mutation probabilities, and individual length. Note that the size, n_c, of the decision variable depends on several factor such as the representation form of $\mathbf{C}_i^q$, the process dimension, the number of control requisites, and the selected controller structure in the previous stage (Eqs. (3)(4)). In this work an integer representation is selected for $\mathbf{C}_i^q \in [0, \min(m, n) - q_o]$ whereby $r = 1$. In this context, the general conditions for running the main algorithm are given and the GA begins the global stochastic search according to the sequential steps described in AppendixB for evolving towards the best suited individuals ($\mathbf{C}_i^d$). It is worth mentioning that the functional cost is evaluated based on the parametrization variable $\mathbf{C}_i = \left[\mathbf{C}_i^d, \mathbf{C}^o\right]$ because it depends on the decision variable $\mathbf{C}_i^d$ as well as the fixed control requisites $\mathbf{C}^o$ (ad-hoc CVs selection). For each iteration in the GA routine, the main problem calls the optimal input-output pairing subproblem of Eq.(10) and described in Section 3.1.1. This subroutine receives a particular subprocess selection called $\mathbf{G}_s$ and returns the optimal pairing $\mathbf{p}_{op}$ by minimizing the RGA-number. The vector $\mathbf{p}_{op}$ contains the column permutation required on $\mathbf{G}_s$ for diagonal pairing. Finally, once the GA code reaches the maximum number of generations the global search stops and the optimal value of additional control loops $\mathbf{C}_{op}^q$, location of selected CVs $\mathbf{C}_{op}^c$, location of selected MVs $\mathbf{C}_{op}^m$, the controller interaction degree $\mathbf{C}_{op}^{\Gamma}$, and the suggested pairing $\mathbf{p}_{op}$ are available for PWC implementation and dynamic simulation testing.

Remark 3: The methodology suggested in this section based on the SSD-NLE combined index gives a more adequate evaluation of the solution space by searching a trade-off solutions between the SSD and NLE indexes. This strategy allows us to focus the exhaustive dynamic simulation tasks to only one optimal PWC design, in contrast, the classical EMSD requires "$\min(m, n) - q_o + 1$ + number of potential pairings + number of controller interaction designs" exhaustive dynamic evaluations to decide. Although both approaches are based on steady-state indexes, it is important to note the strong relationships of such indexes with dynamic character-

istics of the closed loop process. These connections have been analyzed for many researchers the last decades [8, 10, 11, 18, 19, 31, 35].

3.1.1. Automatic input-output pairing based on the RGA number

This section is devoted to summarize the main concepts for implementing the optimal input-output pairing subproblem stated in the constraint Eq. (10). The basic idea is identifying automatically the best diagonal pairing for a given square steady-state matrix $\mathbf{G}_s$ of the process. In this case a GA-based subroutine is proposed by using the well-known RGA-number concept, which can be integrated to the main optimization problem as shown in Eq. (10) as well as in Fig. 2. This index is defined as [8]:

$$\Lambda_n(\mathbf{G}_s) = ||\Lambda(\mathbf{G}_s) - \mathbf{I}||_{\text{sum}}, \tag{15}$$

which gives a measurement of the diagonal dominance of the classical steady-state RGA matrix $\Lambda(\mathbf{G}_s) = \mathbf{G}_s \otimes \left(\mathbf{G}_s^{-1}\right)^T$. The sum-norm is defined as $||\mathbf{A}||_{\text{sum}} = \sum_{ij} |a_{ij}|$ where a_{ij} is the ij-the element of the matrix $\mathbf{A}$.

Original problem: let us consider the vector $\mathbf{p} = [p_1, p_2, \ldots, p_q]$ of positive integer variables. Each component p_i identifies a particular column of the matrix $\mathbf{G}_s$, therefore it must fulfill the following conditions: $p_i \in \mathbb{N}$, $1 \leq p_i \leq q$, and $p_i \neq p_j$ for $i \neq j$. If a particular ordering in the column space of $\mathbf{G}_s$ is called $\mathbf{p}_l$, then the RGA-number can be computed in this case as $\Lambda_n(\mathbf{G}_s(\mathbf{p}_l))$. Hence, an automatic diagonal pairing can be implemented if a suitable columns permutation $\mathbf{p}_l$ is found, such as, the $\Lambda_n(\mathbf{G}_s(\mathbf{p}_l))$ index is minimized.

A simple implementation: in this case a GA-based approach is proposed by using a real positive decision variable $\mathbf{C}_i^p = \left[c_i^{p1}, c_i^{p2}, \ldots, c_i^{pq}\right]$ where each element fulfils $0 \leq c_i^{pj} \leq 1$ with $j = 1, \ldots, q$. Thus, the automatic diagonal input-output paring is given by $\mathbf{p}_i$ in Eq. (16).

$$\min_{\mathbf{C}_i^p} \Lambda_n(\mathbf{G}_s(\mathbf{p}_i)), \quad \text{subject to} \quad \mathbf{p}_i = \text{sort}\left(\mathbf{C}_i^p\right) \tag{16}$$

where the sort function "sort $(\mathbf{C}_i^p)$" reorders the vector $\mathbf{C}_i^p$ in increasing order and returns in $\mathbf{p}_i$ the new position of each element.

This way of computing the optimization over a positive real decision variable $(\mathbf{C}_i^p)$ for subsequently perform a rounding tasks $(\mathbf{p}_i)$ relaxes the original combinatorial problem and improves the GA probability to find valid solutions. This behavior is mainly given by the dimension and the continuous characteristics of the searching space where the mating, crossover, and mutation functions evolve in a more robust manner.

4. Alternative application: DOF changes and PWC redesign analysis

The methodology proposed in section 3.1, is particularly interesting because it is well suited to handle any potential modification of the PWC problem context, i.e. degrees of freedom (DOF) changes. In fact, it allows

a quickly global redesign analysis about the CVs, MVs, controller size and interaction, and input-output pairing if the combinatorial optimization modifies its definition.

Basically, the main root causes of the process DOF modifications are: 1- changes in the number and type of the active constraints and 2- modifications of the controlled process information structure [32]. The active constraint definition, in the first category, may change due to expected or unexpected modifications in the process operation itself, i.e. the real time optimizer decides to fix some particular variable or some process variable reaches its safety limit. The second set involves structural process faults. In this work, the analysis is focused on the latter case, i.e. faults or failures in the process elements such as sensors and/or actuators. Even though there are differences among fault, failure, and malfunction concepts [36], in this work, it is considered that those meanings are unified and represent a particular temporal event from which some process devices lose their functionality suddenly. More specifically, a complete loss is considered in the measurement and actuation devices [37].

In the following paragraphs the potential sensor and actuator faults are integrated to the PWC context. Obviously, the new DOF scenario is characterized via healthy devices, i.e. hardware redundancy-based redesign analysis [38]. When these faults occur the original process can be represented as,

$$\begin{aligned} \mathbf{y}_{f_i}(s) &= \mathbf{G}_{f_{ij}}(s)\mathbf{u}_{f_j}(s) + \mathbf{D}_{f_i}(s)\mathbf{d}(s) \\ \mathbf{G}_{f_{ij}}(s) &= \mathbf{T}_s^i \mathbf{G}(s)\mathbf{T}_a^j \\ \mathbf{D}_{f_i}(s) &= \mathbf{T}_s^i \mathbf{D}(s) \end{aligned} \tag{17}$$

where $\mathbf{G}_{f_{ij}}(s)$ and $\mathbf{D}_{f_i}(s)$ are the matrices associated with the new process representation when the sensor i and the actuator j were lost, i.e. the fault f_{ij} occurs. Indeed, the matrices $\mathbf{T}_s^i$ and $\mathbf{T}_a^j$ are selection matrices which allow to incorporate the i-th and j-th sensor and actuator faults, respectively. The vectors called $\mathbf{y}_{f_i}(s)$ and $\mathbf{u}_{f_j}(s)$ represent all the available healthy sensors and actuators, respectively. On the other hand, the structure of the selection matrices are displayed in Eq. (18). The null column/row represents the i-th/j-th faulty sensor/actuator to be deleted from the original process model. In the fault-free (ff) case the matrices $\mathbf{T}_s^i$ and $\mathbf{T}_a^i$ are replaced by $\mathbf{T}_s^{ff} = \mathbf{I}_{(m\times m)}$, $\mathbf{T}_a^{ff} = \mathbf{I}_{(n\times n)}$, respectively and the approach is the same as section 3.1.

$$\mathbf{T}_s^i = \left[\begin{array}{c|c|c} \mathbf{I} & \begin{matrix}0\\ \vdots\end{matrix} & \mathbf{0} \\ \hline \mathbf{0} & \begin{matrix}\vdots\\ 0\end{matrix} & \mathbf{I} \end{array}\right]_{(m-1)\times m}, \quad \mathbf{T}_a^i = \left[\begin{array}{cccc} \mathbf{I} & & & \mathbf{0} \\ \hline 0 & \cdots & \cdots & 0 \\ \hline \mathbf{0} & & & \mathbf{I} \end{array}\right]_{n\times(n-1)} \tag{18}$$

In this context, the procedure shown in Eqs. (5)-(14) is modified and replaced for the following optimization scenario,

$$\min_{\mathbf{C}_k^{f_{ij}}} \left[\mathrm{SSD}_{\mathbf{y}_r}^{f_{ij}}(\mathbf{C}_k^{f_{ij}}) + \mathrm{NLE}_{\Gamma}^{f_{ij}}(\mathbf{C}_k^{f_{ij}})\right], \tag{19}$$

subject to

$$\left[\begin{array}{l} \mathbf{G}_{f_{ij}} = \mathbf{T}_s^i \mathbf{G} \mathbf{T}_a^j,\ \mathbf{D}_{f_i} = \mathbf{T}_s^i \mathbf{D} \\ \mathbf{G}_s = \mathbf{G}_{f_{ij}} \left([\mathbf{C}_k^c, \mathbf{C}_{f_{ij}}^o], \mathbf{C}_k^m \right),\ \mathbf{D}_s = \mathbf{D}_{f_i} \left([\mathbf{C}_k^c, \mathbf{C}_{f_{ij}}^o] \right) \\ \text{Eqs. (6)-(14)} \end{array}\right. \tag{20}$$

where $\text{SSD}^{f_{ij}}$ and $\text{NLE}^{f_{ij}}$ indicate that the sum of square deviations and the net load evaluation indexes are computed by considering the current i-th sensor and j-th actuator faults f_{ij}, respectively. Note that $\mathbf{C}_k^{f_{ij}}$ is defined as Eq. (3), but in this case $\mathbf{C}_{f_{ij}}^o$ indicates that the original control requisites could be affected by the fault f_{ij}, i.e. particularly when sensor faults occur for the ad-hoc selected CVs.

4.1. Comments on reconfigurable PWC

The methodology suggested in previous section allows to easily reevaluate, off-line, the PWC structure when the DOF scenario changes. The main objective is identifying if additional hardware redundancies are needed for guaranteeing the overall process operability, how the control structure needs to be modified, and finally testing these new control policies based on dynamic simulations. It is clear that all the abnormal events have different effects on the controlled process, so the changing DOF analysis can be made only for the most critical ones, i.e. for those events which produce the process shutdown.

For these particular contexts some emergency/auxiliary control loops can be turned on with the aim to tolerate some critical abnormal events. Tolerance describes the notion of trying to contain the consequences of faults such that the process remains operative. The hardware redundancy plays a crucial role to perform such desirable characteristic [36, 37]. Although the main idea in this work is not to develop a complete on-line fault-tolerant control system, the information given by the methodology suggested in the previous section can be used to develop backup (emergency/auxiliary) control loops for some particular events. In fact, the well-known override/selective controllers are common in industrial practice and they have been used for decades. Indeed, override control applications include: protecting process equipment, automatic startup/shutdown, protection against instrument faults, and signals selections [33, 39, 40].

It is worth mentioning that specific details about the on-line reconfiguration, synchronization, selection logic, and anti-reset windup procedures tied directly to the override control design are beyond the scope of the current work, so will not discussed here.

5. The Tennessee Eastman Process

The case study selected in this work, for testing the previously suggested approaches, is the well-known Tennessee Eastman process (TEP). This plant was introduced by Downs and Vogel [21] as a multivariable nonlinear benchmark for the process control community. Although the original TEP version was modeled in Fortran, the current work is based on the Matlab dynamic simulator generated by compiling the source

code which is available from the Prof. Ricker's web page [22]. The process consists of five major units the reactor, the product condenser, a recycle compressor, a vapor-liquid separator, and a product stripper. The plant produces two liquid products G and H from four gaseous reactants called A, C, D, and E, where also present are an inert B and a byproduct F. The reactions in Eq. (21) are approximately first-order with respect to the reactant concentrations, irreversible, and exothermic.

$$\begin{aligned} \mathrm{A(g)} + \mathrm{C(g)} + \mathrm{D(g)} &\rightarrow \mathrm{G(liq)}, \quad \text{Product 1}, \\ \mathrm{A(g)} + \mathrm{C(g)} + \mathrm{E(g)} &\rightarrow \mathrm{H(liq)}, \quad \text{Product 2}, \\ \mathrm{A(g)} + \mathrm{E(g)} &\rightarrow \mathrm{F(liq)}, \quad \text{Byproduct}, \\ 3\mathrm{D(g)} &\rightarrow 2\mathrm{F(liq)}, \quad \text{Byproduct}. \end{aligned} \tag{21}$$

This plant summarizes 12 available MVs, 41 potential measurements, 20 disturbance scenarios, and six potential operating modes which define several product G/H mass ratios and rates. The most popular operating condition is the base case or mode I where it is required 50/50 mass ratio and 7038 kg/h for G and H rates.

The TEP is an open-loop unstable plant, so a stabilizing control structure is required before applying the approaches discussed in previous sections. In this work, the stabilizing control policy opportunely suggested by McAvoy and Ye [23] is adopted, which consists of flow (inner) and level (cascade) controllers for the reactor, separator, and stripper. Figure 3 shows the TE process layout and the corresponding stabilizing control structure.

The main scenario considered here for PWC design is shown in Table 2 and corresponds to the working point identified as the base case, with $m = 12$ outputs, $n = 8$ inputs, and $p = 2$ disturbances. The same framework was used in previous publications of the author [18, 19]. According to the definitions stated in section 2 the overall PWC problem belongs to the **Case II** with its corresponding functional cost. This table summarizes the connection between the nomenclature used here (first column) and the description used opportunely in the precursory work (last column). Furthermore, the original control requisites stated by Downs and Vogel [21] define that the output variables identified as y_9, y_{10}, y_{11}, and y_{12} need be controlled and this fact is indicated with an asterisk in Table 2.

Once the PWC is designed and implemented, the final testing is performed on the nonlinear dynamic simulator by considering the following challenging scenarios stated by Downs and Vogel [21]:

- Set point changes:
  - $XME(7)$: Reactor operating pressure step change from 2705 to 2645 kPa.
  - $XME(17)$: Production rate step change from 14.228 to 12.094 kg/h.
  - $XME(30)$: B composition in purge step change from 13.82 to 15.82 %.
  - $XME_{G/H}$: Product mix step change from 50 G/50 H to 40 G/60 H.

called here sp1, sp2, sp3, and sp4.

- Disturbances:
  - $IDV1$: A/C feed ratio step change, B composition constant (stream 4).
  - $IDV2$: B composition step change, A/C ratio constant (stream 4).
  - $IDV4$: Reactor cooling inlet temperature step change.
  - $IDV8$: A, B, C feed compositions random changes (stream 4)
  - $IDV12/IDV15$: Condenser cooling water inlet temperature random changes and condenser cooling water valve sticking.

  called here d1, d2, d3, d4, and d5.

6. Results and discussion

This section is devoted to display the main results of the new SSD+NLE combined index approach suggested in sections 3.1 and 4 on the TEP. These results and discussions are divided in three major sections for a proper analysis and comparison. Initially, the SSD+NLE combined index approach is applied and the new PWC suggested is further evaluated dynamically against the classical EMSD methodology [19] to show the improvements. Abnormal events or structural faults were not considered in this first evaluation, i.e. a fault-free design context. The second main section is related to display the PWC redesign analysis concepts stated in section 4, i.e. changes in DOF conditions. The basic idea here is to analyze how the optimal PWC structure, designed in the fault-free scenario, behaves under structural process faults and evaluate if some emergency (backup) control loops could be useful to guarantee the overall process operability. Finally, a discussion is presented by comparing the suggested approach and the final PWC structure with some earlier works in the area.

It is worth mentioning that, for simplicity, all the PWC structures considered here are decentralized ones, i.e. several SISO (single input-single output) control loops without interaction. Hence, the controller structure is diagonal with $\Gamma = \mathbf{I}$ and the parametrization $\mathbf{C}_i^{\Gamma}$ is not used in Eq. (3).

6.1. Classical EMSD and SSD-NLE combined index approaches

Remembering the discussion in the previous section, the PWC design scenario is defined by $q_o = 4$ original control requisites (ad-hoc CVs selection), $m = 12$ outputs, $n = 8$ inputs, $p = 2$ disturbances, and $v = 7$ stabilizing control loops. Moreover, considering the combinatorial problem size stated in section 2, for the **case II**, there are $[(m-q_o)!/(q_a!(m-q)!)][n!/(q!(n-q)!)] = 1820$ feasible PWC solutions. This number increases even more if we consider all the potential input-output pairings, hence it is clear that an heuristic evaluation of these solutions results unpractical.

The classical EMSD approach shown in Fig. 1 and suggested by Zumoffen [19] represents a systematic and generalized methodology to avoid the exhaustive evaluation of these 1820 potential solutions. Indeed, the classical EMSD strategy focuses mainly on $\max(q_a)+1=5$ potential optimal PWC structures, where $0 \leq q_a \leq \min(m,n)-q_o=4$, which shows a remarkable reduction in the problem size. Anyway, for deciding about the final control policy, the five control structures ((11×11) to (15×15)) need to be implemented and their performances tested dynamically on the non linear simulator. A complete analysis is performed in Zumoffen [19] and the final conclusion is that the PWC structure with dimension (12×12) presents the best trade-off behavior between the integral absolute tracking error (IAE) for the main process variables and the operating cost.

The modification suggested in section 3.1, the SSD-NLE combined index, facilitates the final selection of the multi-loop control structures by minimizing the dynamic simulations burden and the heuristic knowledge requirements. The methodology suggested in Eqs. (5)-(14) is applied to the TEP with the same scenario as defined at the beginning of this section, $\mathbf{C}^o=[1\,1\,1\,1]$, $q_o=4$ and $0\leq q_a\leq 4$. The parametrization variable results $\mathbf{C}_i=[\mathbf{C}_i^q,\mathbf{C}_i^c,\mathbf{C}^o,\mathbf{C}_i^m]$ where each subcomponent has the following dimensions (1×1), $(1\times(m-q_o))$, $(1\times q_o)$, and $(1\times n)$, respectively. In this case, $\mathbf{C}_i^q$ is an integer decision variable into the q_a range and $\Gamma=\mathbf{I}$. The corresponding optimization problem is solved here by using the GA approach with the parameter settings displayed in Table 3 (see AppendixB). Note that in this context the overall combinatorial problem dimension is $(5^1)(2^{16})=327680$, with only $[(m-q_o)!/(q_a!(m-q)!)][n!/(q!(n-q)!)]=1820$ feasible solutions according to $0\leq q_a\leq \min(m,n)-q_o=4$. On the other hand, the optimization time to solve this problem was ≈ 1.8 hours (Intel Core, i5-2400, 3.1 GHz, 3 GB RAM).

The SSD-NLE combined index approach allows us to focus all our attention on just one solution, reducing even more the overall problem size. Indeed, the PWC suggested in this case is called OPWC_3 and it is shown in Table 4. This solution represents a control policy of (13×13) decentralized controllers (6 servo/regulatory and 7 stabilizing control loops). Furthermore, Table 4 also summarizes two additional PWC structures named OPWC_1 and OPWC_2 which come from the classical EMSD methodology and they have been used here for dynamic comparison purposes. The overall description of these control policies are the following:

- OPWC_1: the best (12×12) solution suggested by the classical EMSD approach [19] with $q_a=1$. Best pairing: u_1-y_{12}, u_2-y_9, u_3-y_{10}, u_5-y_{11}, u_7-y_8.
- OPWC_2: the best (13×13) solution suggested by the classical EMSD approach [19] with $q_a=2$. Best pairing: u_1-y_{12}, u_2-y_9, u_3-y_{10}, u_4-y_8, u_5-y_{11}, u_7-y_1.
- OPWC_3: the (13×13) optimal policy suggested by the modified methodology with $q_a=2$. Best pairing: u_1-y_{12}, u_2-y_9, u_3-y_{10}, u_5-y_{11}, u_7-y_2, u_8-y_7.

It is worth mentioning the main differences about the number, type and pairing of the variables for the

three PWC structures to be compared. This fact impacts directly in the SSD+NLE index shown in the last column in Table 4. In theory, the control structure called $OPWC_3$ presents the best servo/regulator performance, i.e. better dynamic behavior. This fact will be tested dynamically on the non linear simulator benchmark.

The dynamic performances for $OPWC_1$, $OPWC_2$, and $OPWC_3$ control policies are summarized in Fig. 4 and Fig. 5. The integral absolute tracking error (IAE) between the CV and its corresponding reference trajectory for the main process variables are shown in Figs. 4(a)(b), which correspond to the reactor pressure (y_9) and B composition in purge and (y_{11}), respectively. All the scenarios, sp1 to sp4 and d1 to d5, are considered here for comparing the three PWC structures. It is clear that the new control policy suggested by the modified EMSD methodology, $OPWC_3$, considerably improves the servo/regulator behavior for the scenarios called sp2, sp3, d1, d2, d4, and d5. Some scenarios where the $OPWC_3$ structure presents notable improvements are summarized dynamically along 70 hr of simulation time in Fig. 5. In fact, the temporal evolution of the reactor pressure when disturbance d1 occurs and the profile of the B composition in purge when disturbance d2 is present are shown in Fig. 5(a) and Fig. 5(b), respectively. In both cases the disturbance effect appears at $t = 0$ hour. It is clear that the new $OPWC_3$ policy allows maintaining the reactor pressure under normal operating limits, improving the response time and reducing the variability. On the other hand, the settling time and the peak values are drastically reduced in the purge composition.

The significant improvements introduced by the $OPWC_3$ structure rely on the new methodology based on combined SSD-NLE index. Indeed, this modified version of the EMSD approach allows to design PWC structures focused on minimizing the SSD index for the UVs as well as reducing the NLE among CVs when servo/regulator behavior is assumed for the diagonal controller. Moreover, the suggested approach explores the correct controller size.

6.2. PWC redesign analysis: sensor faults

In previous section an optimal PWC structure, called $OPWC_3$, was designed based on the SSD-NLE combined index approach for the fault-free scenario. This control policy is named here $OPWC_{\text{ff}}$ highlighting this fact.

The basic idea here is analyzing how this nominal PWC behaves when some components lose functionality (structural faults) and evaluate if some kind of PWC redesign (backup/emergency/auxiliary control loop) could be useful to guarantee the overall process operability. The main concepts from section 4 are used here.

Without loss of generality, only faults in sensors are considered due to both simplicity and space issues. Remembering the Table 4, the control policy $OPWC_{\text{ff}}$ requires six sensors $[y_2, y_7, y_9, y_{10}, y_{11}, y_{12}]$ for the servo/regulatory control layer. Hence, the first aim is to analyze the overall behavior of the closed-loop process when those sensors are lost. Table 5 summarizes the effects produced by the mentioned six sensor faults f_1 to f_6 (the second column shows the corresponding faulty measurement) on the $OPWC_{\text{ff}}$ control

structure when all the simulation scenarios were considered. When the fault f_i $(i = 1, \ldots, 6)$ occurs, the feedback information given by the y_j $(j = 2, 7, 9, 10, 11, 12)$ output measurement is lost, hence the corresponding control loop works in open-loop manner. This means that the optimal control policy OPWC_{ff} loses one control loop and therefore its optimality. The control structure formed by the remaining healthy control loops are called in this case FPWC_{fi}, i.e. a faulty PWC structure. The symbolism used in that table is the following: "✓" defines a stable operation condition, "⊗" means that this setpoint change cannot be implemented due to the loss of the respective sensor, and "SD" represents the shutdown of the process operation due to violations of the operating limits. Note that the SSD+NLE index value is also displayed in each scenario.

The faults called f_2, f_4, and f_6 do not produce any drastic process condition and the plant operability is guaranteed. The corresponding SSD+NLE indexes are very close to the fault-free case (≈ 19.76 in Table 4). It is important to note that, in these cases, while a stable operation is maintained, by the remaining operative control loops, the performance in some process variables may be reduced due to the lack of a complete control structure. For these faults no PWC redesigns (emergency control loops) are required, so the overall process behavior it is assumed acceptable. The faults set highlighted with gray background, f_1, f_3, and f_5, leave the process inoperative producing the mentioned shutdown of the plant for scenarios d1, d2, and sp4. Note that the SSD+NLE indexes are deviate considerably from the fault-free case. Generally, this undesired shutdown generates enormous monetary losses due to unsold products and the costs involved in re-startup of the plant. Eventually, legal problems may also occur due to out-of-specification operation in some units.

For avoiding these drastic scenarios the methodology suggested in section 4 is used here for analyzing potential PWC redesigns based on auxiliary/emergency control loops. In fact, control policies are reevaluated for the f_1, f_3, and f_5 faulty scenarios. Table 6 shows the new control structures suggested for guaranteeing the process operability which are called OPWC_{f1}, OPWC_{f3}, and OPWC_{f5}, respectively. The last column of this table summarizes the new SSD-NLE index values for these structures. Remembering the faulty values of Table 5, in these case an improvement of 28.79, 63.88, and 35.40 % can be identified, respectively. Comparing Table 6 with the fault-free PWC design OPWC_{ff} shown in Table 4, the following differences can be discussed:

- OPWC_{f1}: when the reactor feed flow sensor is lost (y_2), this new structure suggests to add the recycle flow sensor (y_1) and controlling this variable via the same manipulated variable, the reactor colling water inlet temperature set point (u_7). The new loop is reasonable because either y_1 or y_2 can be used to fix the recycle flow to the reactor. This auxiliary control loop can be implemented based on the override control theory on OPWC_{ff} to guarantee operability of the process.

- OPWC_{f3}: in this case the reactor pressure sensor (y_9) is lost, and this new control structure suggest to include the stripper pressure sensor (y_6) and controlling this variable with the same input, i.e. the A

feed flow (u_2). This auxiliary loop seems to be reasonable because the reactor, stripper and separator pressures are strongly correlated, so any of them can be used to fix the remaining ones. Again here an override control procedure can be implemented for security issues.

- OPWC_{f5}: when the B composition in purge sensor (y_{11}) is lost, this new structure suggests to incorporate the compressor work sensor (y_8) and controlling this variable with the same manipulated one, i.e. the purge valve (u_5). Furthermore, this structure also proposes that the stripper temperature (y_7) needs to be controlled via the stripper steam valve (u_6) instead of the condenser cooling water flow (u_8). Both auxiliary control loops can be implemented based on override or selective control configuration.

The control structure called OPWC_{ff} (or OPWC_3) is displayed in Fig. 6, where indicators and controllers are represented with white circles. Furthermore, on the same figure also are implemented the mentioned override controllers for handling the most drastic faults (in this case f_1, f_3, and f_5). These selective controllers and its corresponding indicators are represented via gray filled circles.

Display the dynamic behavior of the main process variables (y_9, y_{10}, y_{11}, and y_{12}) for all the scenarios and control structures summarized in Table 5 and Table 6 results totally prohibitive as well as impractical. Instead, only the temporal profiles for the most critical scenarios are shown in Fig. 7 where the reactor pressure is presented. Figures 7(a) to 7(c) compare the control policies called: fault-free OPWC_{ff}, faulty case FPWC_{fi}, and the reconfigured OPWC_{fi} structure when the fault fi occurs at $t = 10$ hours with $\text{fi} = \text{f1}, \text{f2}, \text{f3}$, respectively. The disturbances and reference changes selected in each case are those presented in Table 5 which identify a process shutdown (SD). It is clear here that, the backup control loops suggested by each control structure called OPWC_{f1}, OPWC_{f3}, and OPWC_{f5} guarantee the overall process operability and allow to operate the plant very close to the normal case identified with OPWC_{ff}. The shutdown time for the all cases is named t_{SD}.

6.3. Comments on related works

There are several PWC proposals in literature for the Tennessee Eastman process developed in the most varied scenarios and by using the most varied methodologies. In this context an exhaustive comparison becomes complex, incomplete or impossible for some approaches. Some comments related to the general classification into heuristic-based, mathematical-based, or hybrid-based approaches were given in section 1.3. Due to the diverse range of existing control structures with similar dynamic performances, the main comparison tasks are focused on structural resemblances and hardware requirements among them. Particularly, the concept of hardware requirements is related to the total number of measurements (TM), control loops (CL), and compositions required to be measured (CM). Indeed, the most relevant applications are summarized in the following.

A precursory PWC design was proposed by McAvoy and Ye [23] (TM: 22, CL: 22, CM: 4). The multi-loop control structure, for the base case TEP, is developed based on heuristic considerations with focus on the plant operability even if the analyzers are not functioning. Some special scenarios require to design specific override controllers such as reactor pressure (y_9)–purge valve (u_5) plus a cutting-back the production (lower A/C feed flow). The work of Lyman and Georgakis [24] (TM: 20, CL: 20, CM: 5) is based on the tired approach for heuristic multi-loop control structure design. Paradoxically, this proposal does not use the reactor pressure as a CV, which is an ad-hoc requisite by Downs and Vogel [21]. Several scenarios were run with a reduction of 15% in the production rated, basically for avoiding shutdown problems. Furthermore, an override controller is proposed to switch the classic B composition in purge (y_{11})-purge valve (u_5) control loop to C composition in purge-purge valve (u_5). The production rate (y_{10}) in this case is suggested to be controlled by the condenser cooling water flow (u_8). On the other hand, Ricker [25] (TM: 17, CL: 19, CM: 3) proposes a very complex PWC design based on heuristics, feedback, feedforward, ratio, and override control for the TEP at the optimal operating point. All the flows in the process are controlled by ratio control with the production rate. Two overrides controllers were proposed to guarantee a safety operation: 1- if the reactor pressure y_9-purge valve (u_5) control loop saturates, the production rate set point is used as backup and then lowered and 2- the reactor level- condenser cooling water flow (u_8) is switched to the recycle valve (u_4) as a backup. The production rate changes were fixed as ramp for avoiding large transients and saturation problems. The heuristic nine steps approach is applied in Luyben et al. [26] (TM: 19, CL: 20, CM: 2) for decentralized control design at the base case. In this case five (5) override controllers were suggested to guarantee operability of the process in some scenarios. Indeed, override control in purge flow, D feed flow, and the three levels change their MVs. In this case the A feed flow (u_2) is used to control the A composition in the purge and eventually the reactor pressure is controlled by the A/C feed flow (u_3), leaving the production rate to be fixed by the stripper underflow. On the other hand, Larsson et al. [29] (TM: 22, CL: 19, CM: 3) propose a design based on the self-optimizing ideas and the inner cascade flow controllers suggested by Ricker [25]. The main idea here is the controlled variable selection by using all the DOF available. Some disturbance scenarios are avoided because they require to design several override controllers, which they were not designed in this work. Recently, Jha and Okorafor [9] (TM: 20, CL: 21, CM: 6) propose a new control policy by integrating self-optimizing concepts, steady-state simulation, and mathematics-based analysis similar to the IF approach of Vasudevan et al. [30]. The overall structure has some problems to reject properly some disturbances. Indeed, three override control structures were proposed: 1- B comp purge (y_{11})–purge valve (u_5) to purge fully open for problems with reactor pressure, 2- reactor pressure y_9–A/C feed flow (u_3) to C composition in reactor feed–A/C feed flow, and 3- for some setpoints changes reactor feed composition control switch to product rate and quality control.

Although all the above mentioned proposals suggest valid PWC structures, it is clear that the hardware requisites and the application range is really varied. The SSD-NLE combined index approach proposed here

gives excellent and reliable designs, from the hardware requisites point of view (TM: 13, CL: 13, CM: 3), by analyzing all the searching space properly and avoiding oversizing problems. Furthermore, the integrated index improves the closed-loop behavior respect to previous work of the author such as Molina et al. [18] (TM: 15, CL: 15, CM: 3) and Zumoffen [19] (TM: 12, CL: 12, CM: 3).

7. Conclusion

In this work an alternative methodology called SSD-NLE comnbined index approach was presented for multi-loop control structure design. The overall strategy is based on a single multi-objective combinatorial optimization problem with steady-state functional costs. This proposal allowed us to properly address typical PWC drawbacks such as the ad-hoc reduction of the problem size, all the available DOF are used and fixed, the reduced information about the process limits the design stage, and the control policies are only focused on decentralized control.

This mathematical representation allows considering the original size of the problem without any ad-hoc reduction, furthermore any a priori heuristic consideration may be included properly via weighting matrices. The unified programing suggested here consists of two steady-state contributions called the sum of square deviations (SSD) and the net load evaluation (NLE) indexes, which have strong connection with the controllability/performance properties of the current PWC. This new optimization problem allows to define the CVs, MVs, controller order/size, the input-output pairing, and the controller interaction, simultaneously. Hence, several different DOF may be evaluated and no dynamic models are needed in this design stage. This feature generalizes and systematizes the overall PWC design procedure focusing the search to simple feedback control structures. Moreover, the NLE component gives relevant information related to the controller interaction and how this structure affects the closed-loop performance. Thus, if required, integrated multi-loop control policies can be designed eventually as base structure. Furthermore, an alternative application of the SSD-NLE comnbined index approach was proposed when the DOF change due to structural process faults such as sensor and/or actuator malfunctions. This methodology gives a reliable PWC redesign analysis by defining multiple security/stability control loops for guaranteeing the process operability (based on the hardware redundancy theory). Moreover, this kind of control loops can be easily implemented via the override/selective controller concepts from industrial practice.

It is worth mentioning that the proposed methodology for PWC design is mainly focused to control structure design and evaluation from the conceptual engineering point of view. The main real application is to analyze (off line) potential PWC structures, how the performance of these policies are affected by eventual structural process faults, and if hardware redundancy could be useful in some extent. Thus, relevant information can be obtained, for example, for the process synthesis and design stage.

Acknowledgements

The authors thank the financial support of CIFASIS-CONICET, ANPCYT (PICT 2012-0133), and UTN-FRRo from Argentina. The authors also acknowledge the valuable contribution of Dr. Alejandro Marchetti and Dr. Diego Feroldi in the review process.

AppendixA. SSD and NLE approaches

Remembering that in Eq. (2) a control structure with integral action was implemented, then at steady state ($s = 0$) we have $\mathbf{y}_s = \mathbf{y}_s^{sp}$ and,

$$\begin{aligned} \mathbf{u}_s &= \mathbf{G}_s^{-1}\mathbf{y}_s^{sp} - \mathbf{G}_s^{-1}\mathbf{D}_s\mathbf{d}, \\ \mathbf{y}_r &= \mathbf{G}_r\mathbf{G}_s^{-1}\mathbf{y}_s^{sp} + \left(\mathbf{D}_r - \mathbf{G}_r\mathbf{G}_s^{-1}\mathbf{D}_s\right)\mathbf{d} = \mathbf{S}_{sp}\mathbf{y}_s^{sp} + \mathbf{S}_d\mathbf{d}, \end{aligned} \tag{A.1}$$

it can be observed that both MVs and UVs deviations depend on the selected square subprocess $\mathbf{G}_s$ and if the setpoint and disturbance effects are considered individually, then, the SSD index (for UVs in this case) can be stated as

$$\mathrm{SSD}_{\mathbf{y}_r} = ||\Lambda_2\mathbf{S}_{sp}\Lambda_1||_F^2 + ||\Theta_2\mathbf{S}_d\Theta_1||_F^2\,, \tag{A.2}$$

where diagonal weighting matrices Λ_1 $(n \times n)$ and Θ_1 $(p \times p)$ allow to include the process control objectives such as setpoint/disturbance magnitudes (this is important when the used process model is not normalized). Similarly, Λ_2 $((m-n)\times(m-n))$ and Θ_2 $((m-n)\times(m-n))$ take into account the relative degree of importance among the overall outputs. In addition, $||\cdot||_F$ means the Frobenius norm for matrices.

The selected subprocess $\mathbf{G}_s$, which minimizes either $\mathrm{SSD}_{\mathbf{y}_r}$ or $\mathrm{SSD}_{\mathbf{u}_s}$, is well-conditioned and has good controllability properties. An exhaustive analysis can be found in Molina et al. [18] and Zumoffen and Basualdo [31].

On the other hand, considering the CVs expression in Eq. (2) and the IMC control structure we have

$$\mathbf{y}_s(s) = \mathbf{F}(s)\mathbf{y}_s^{sp}(s) + (\mathbf{I} - \mathbf{F}(s))\mathbf{y}_s^{net}(s) \tag{A.3}$$

$$\mathbf{y}_s^{net}(s) = \mathbf{A}_n(s)\mathbf{y}_s(s) + \mathbf{B}_n(s)\mathbf{d}(s) \tag{A.4}$$

$$\mathbf{A}_n(s) = \left[\mathbf{I} + \left(\mathbf{G}_s(s) - \tilde{\mathbf{G}}_s(s)\right)\mathbf{G}_c(s)\right]^{-1}\left(\mathbf{G}_s(s) - \tilde{\mathbf{G}}_s(s)\right)\mathbf{G}_c(s) \tag{A.5}$$

$$\mathbf{B}_n(s) = \left[\mathbf{I} + \left(\mathbf{G}_s(s) - \tilde{\mathbf{G}}(s)\right)\mathbf{G}_c(s)\right]^{-1}\mathbf{D}_s(s). \tag{A.6}$$

The CVs are affected by $\mathbf{y}_s^{net}(s)$ in the transient because the term $\left(\mathbf{I} - \tilde{\mathbf{G}}_s(s)\mathbf{G}_c(s)\right)$ produces integral action at steady-state. The harmful effects in the transient are directly related to the multivariable gain of $[\mathbf{A}(s)\mathbf{B}(s)]$ and the time constants of the diagonal low-pass TFM $\mathbf{F}(s)$. Because the filter setting cannot be chosen freely, the only way to reduce these effects in the CVs is by reducing the deviations of $\mathbf{y}_s^{net}(s)$ in a

sum of square sense, then the net load evaluation (NLE) results:

$$\text{NLE}_\Gamma = \|\Delta_2 \mathbf{A}_{n\Gamma} \Delta_1\|_F^2 + \|\Xi_2 \mathbf{B}_{n\Gamma} \Xi_1\|_F^2 \tag{A.7}$$

with

$$\mathbf{A}_{n\Gamma} = \mathbf{I} - \tilde{\mathbf{G}}_{s\Gamma} \mathbf{G}_s^{-1},\ \mathbf{B}_{n\Gamma} = \tilde{\mathbf{G}}_{s\Gamma} \mathbf{G}_s^{-1} \mathbf{D}_s,\ \tilde{\mathbf{G}}_{s\Gamma} = \mathbf{G}_s \otimes \Gamma,\ \Gamma = \begin{bmatrix} \gamma_{11} & \cdots & \gamma_{1n} \\ \vdots & \ddots & \vdots \\ \gamma_{n1} & \cdots & \gamma_{nn} \end{bmatrix}, \tag{A.8}$$

where $\mathbf{A}_{n\Gamma}$ and $\mathbf{B}_{n\Gamma}$ are the net load matrices shown in Eqs. (A.5) and (A.6) at steady state and parameterized with the process model selection $\tilde{\mathbf{G}}_{s\Gamma}$ displayed in Eq. (A.8). Note that γ_{ij} belongs to the binary alphabet $\{0, 1\}$ indicating the selection ($\gamma_{ij} = 1$) or not ($\gamma_{ij} = 0$) of the ij process element and $\otimes$ is the Hadamard product. On the other hand, Δ_1, Δ_2, Ξ_1 and Ξ_2 are diagonal weighting matrices which allow to sort the process control objectives according to its relative importance in the system, specially when the used process model is not normalized.

The minimization of NLE_Γ gives the optimal Γ which parameterizes the plant-model mismatch and the controller interaction $\mathbf{G}_c(s) = \tilde{\mathbf{G}}_{s\Gamma}^{-1}(s)\mathbf{F}(s)$. Thus, $\mathbf{G}_c(s)$ represents the optimal controller which minimizes the effects of $\mathbf{y}_s^{net}(s)$ in the CVs. A detailed description of these topics can be found in Molina et al. [18], Zumoffen and Basualdo [31], and Zumoffen et al. [41].

AppendixB. Genetic algorithms

Genetic algorithms (GA) represent a well-known methodology to perform a stochastic global search (optimization) by simulating the metaphor of the real biological evolution. Mainly, GA operate on a population of individuals (potential solutions) which are evaluated, selected, merged, mate, and mutate (operators borrowed from natural genetics) along the generations in order to find the best population according to some particular environment (fitness function) [34].

The classical steps involved in any GA-based optimization methodology are shown in Algorithm 1. The initialization phase summarizes all the data required for starting the algorithm: the initial population $\mathbf{P}_0$ (where n_i individuals with length n_c are generated randomly), the maximum allowed generation n_g, the amount of individuals to be selected $n_s = n_i/2$, and the reproduction and mutation probabilities p_c and p_m, respectively. The first evaluation is the criterion for stoping the overall procedure, i.e. the maximum allowed generations. The following step is the fitness evaluation $f(\mathbf{C}_i^d)$ by considering all the individuals in the current population $\mathbf{P}_j$. In this stage, the best individual is stored in the best population set $\mathbf{P}_b$ and its value in the vector $\mathbf{F}$. The individuals selection is performed by means of some stochastic operator, i.e. roulette wheel method, according to their relative fitness values. In this context, the best $n_s = n_i/2$ individuals are retained in $\mathbf{P}_s$ and the remaining ones are discarded. The production of new chromosomes from $\mathbf{P}_s$

is developed by the crossover or recombination operators, i.e. double-point method, with a probability p_c and stored in the new matrix $\mathbf{P}_r$. Analogously to the natural evolution, the mutation produces a new genetic structure and basically is applied with a low probability p_m. Mutation generally tends to inhibit the possibility of converging to a local optimum [4, 34]. Hence, matrix $\mathbf{P}_r$ is mutated and stored in $\mathbf{P}_m$. Finally, the original selected subpopulation $\mathbf{P}_s$ and the mutated one $\mathbf{P}_m$ are merged (stacked) to give the next generation of individuals, $\mathbf{P}_j = [\mathbf{P}_s^T, \mathbf{P}_m^T]^T$. When $j = n_g$ the termination criterion is true and the overall procedure stops to provide the matrix $\mathbf{P}_b$ $(n_g \times n_c)$ and the vector $\mathbf{F}$ $(n_g \times 1)$, which summarize the set of the best individuals along the generations and their corresponding fitness values, respectively.

References

[1] A. Khaki-Sedigh and B. Moaveni. *Control Configuration Selection for Multivariable Plants*, volume 391 of *Lecture Notes in Control and Information Sciences*. Springer-Verlag Berlin Heidelberg, 2009.

[2] G.P. Rangaiah and V. Kariwala. *Plantwide Control. Recent Developments and Applications*. John Wiley and Sons Ltd, 2012.

[3] J. Downs and S. Skogestad. An industrial and academic perspective on plantwide control. *Anual Reviews in Control*, 35: 99/110, 2011.

[4] M. Sharifzadeh and N. Thornhill. Optimal selection of control structure using a steady-state inverselly controlled process model. *Computers and Chemical Engineering*, 39:126–138, 2012.

[5] G. Stephanopoulos and G. Reklaitis. Process systems engineering: From Solvay to modern bio- and nanotechnology. A history of development, successes, and prospects for the future. *Chemical Engineering Science*, 66:4272–4306, 2011.

[6] P. Buckley. *Techniques of process control*. Willey, 1964.

[7] W. Luyben, B. Tyréus, and M. Luyben. *Plant-wide process control*. McGraw-Hill, 1998.

[8] S. Skogestad and I. Postlethwaite. *Multivariable feedback control. Analysis and Design*. John Wiley & Sons, 2005.

[9] A. Jha and O. Okorafor. Optimal plantwide process control applied to the Tennessee Eastman problem. *Industrial Engineering & Chemistry Research*, 53:738–751, 2014.

[10] P. Grosdidier, M. Morari, and B. Holt. Closed-loop properties from steady-state gain information. *Industrial & Engineering Chemistry Fundamentals*, 24:221/235, 1985.

[11] S. Skogestad and M. Morari. Implications of large RGA elements on control performance. *Industrial & Engineering Chemistry Research*, 26:2323/2330, 1987.

[12] Z. Yuan, B. Chen, and J. Zhao. Effect of manipulated variables selection on the controllability of chemical processes. *Industrial & Engineering Chemistry Research*, 50:7403/7413, 2011.

[13] E. Bristol. On a new measure of interaction for multivariable process control. *IEEE Transactions on Automatic Control*, 1966.

[14] M.J. He, W.J. Cai, W. Ni, and L.H. Xie. RNGA based control system configuration for multivariable processes. *Journal of Process Control*, 19:1036/1042, 2009.

[15] W. Assali and T. McAvoy. Optimal selection of dominant measurements and manipulated variables for production control. *Industrial & Engineering Chemistry Research*, 49:7832/7842, 2010.

[16] V. Alstad and S. Skogestad. Null space method for selecting optimal measurement combinations as controlled variables. *Industrial & Engineering Chemistry Research*, 46:846/853, 2007.

[17] A. Marchetti and D. Zumoffen. Self-optimizing control structures with minimum number of process-dependent controlled variables. *Industrial & Engineering Chemistry Research*, 53:10177—-10193, 2014.

[18] G. Molina, D. Zumoffen, and M. Basualdo. Plant-wide control strategy applied to the Tennessee Eastman process at two operating points. *Computers and Chemical Engineering*, 35(10):2081–2097, 2011.

[19] D. Zumoffen. Oversizing analysis in plant-wide control design for industrial processes. *Computers and Chemical Engineering*, 59:145–155, 2013.

[20] M. Munir, W. Yu, and B. Young. Plant-wide control: Eco-efficiency and control loop configuration. *ISA Transactions*, 52:162–169, 2013.

[21] J. Downs and E. Vogel. A plant-wide industrial process control problem. *Computers and Chemical Engineering*, 17(3): 245–255, 1992.

[22] N.L. Ricker. Data & code archive web page. *Department of Chemical Engineering, University of Washington*. URL http://depts.washington.edu/control.

[23] T. McAvoy and N. Ye. Base control for the Tennnessee Eastman challenge process. *Computers and Chemical Engineering*, 19:453–480, 1995.

[24] P.R. Lyman and C. Georgakis. Plant-wide control of the Tennessee Estman problem. *Computers and Chemical Engineering*, 19:321–331, 1995.

[25] N.L. Ricker. Decentralized control of the Tennessee Estman challange process. *Journal of Process Control*, 6:205–221, 1996.

[26] M.L. Luyben, B.D. Tyreus, and W.L. Luyben. Plantwide control design procedure. *AIChE Journal*, 43:3161–3174, 1997.

[27] Björn D. Tyreus. Dominant variables for partial control. 2. application to the Tennessee Estman challange process. *Ind. Eng. Chem. Res.*, 38:1444–1455, 1999.

[28] N.L. Ricker. Optimal steady-state operation of the Tennessee Estman challange process. *Computers and Chemical Engineering*, 19:949–959, 1995.

[29] T. Larsson, K. Hestetun, E. Hovland, and S. Skogestad. Self-optimizing control of a large-scale plant: the Tennessee Estman process. *Ind. Eng. Chem. Res.*, 40:4889–4901, 2001.

[30] S. Vasudevan, G.P. Rangaiah, N.V.S.N Murthy Konda, and W.H. Tay. Application and evaluation of three methodologies for plantwide control of the styrene monomer plant. *Ind. Eng. Chem. Res.*, 48:10941–10961, 2009.

[31] D. Zumoffen and M. Basualdo. Improvements on multiloop control design via net load evaluation. *Computers and Chemical Engineering*, 50:54–70, 2013.

[32] R. Rhinehart, M. Darby, and H. Wade. Choosing advanced control. *ISA Transactions*, 50:2–10, 2011.

[33] Béla G. Lipták. *Instrument engineers' handbook. Process control and optimization*, volume II. CRC Press. Taylor & Francis Group, 4th edition, 2006.

[34] A. Chipperfield, P. Fleming, H. Pohlheim, and C. Fonseca. Genetic algorithm toolbox. for use with matlab. *University of Sheffield*, 44:5645–5659, 1994. URL http://codem.group.shef.ac.uk/index.php/ga-toolbox.

[35] C. Garcia and M. Morari. Internal model control. 2. design procedure for multivariable systems. *Ind. Eng. Chem. Process Des. Dev.*, 24:472–484, 1985.

[36] R. Isermann. *Fault-Diagnosis Systems. An Introduction from Fault Detection to Fault Tolerance*. Springer-Verlag Berlin Heidelberg, Germany, 2006.

[37] J. Jiang and X. Yu. Fault-tolerant control systems: A comparative study between active and passive approaches. *Annual Reviews in Control*, 36:60–72, 2012.

[38] Y. Zhang and J. Jiang. Bibliographical review on reconfigurable fault-tolerant control systems. *Annual Reviews in Control*, 32:229–252, 2008.

[39] W. Svrcek, D. Mahoney, and B. Young. *A Real-Time Approach to Process Control*. John Wiley & Sons Ltd, 2nd edition, 2006.

[40] F. Manenti. Natural gas operations: considerations on process transients, design, and control. *ISA Transactions*, 51:

317–324, 2012.

[41] D. Zumoffen, G. Molina, and M. Basualdo. Improvements on multivariable control strategies tested on the Petlyuk distillation column. *Chemical Engineering Science*, 93:292–306, 2013.

Nomenclature

Acronyms

CVs: Controlled variables

DOF: Degrees of Freedom

DVs: Disturbances variables

EMSD: Extended MSD

FPWC$_{\text{fi}}$: Faulty PWC for fault f_i

GA: Genetic Algorithms

IAE: Integral Absolute Error

IMC: Internal model control

MSD: Minimum squared deviation

MVs: Manipulated variables

NLE: Net load evaluation

OPWC$_{\text{ff}}$: Optimal PWC fault-free case

OPWC$_{\text{fi}}$: Optimal PWC redesign for fault f_i

PSE: Process Systems Engineering

PWC: Plant-wide control

RGA: Relative Gain Array

SD: Shutdown

SSD: Sum of squared deviations

TEP: Tennessee Eastman Process

TFM: Transfer functions Matrix

UVs: Uncontrolled variables

Variables

$\mathbf{A}_n(s)$: Net load TFM - Set point effect

$\mathbf{A}_{n\Gamma}$: Steady-state $\mathbf{A}(s)$ parameterized with Γ

$\mathbf{B}_n(s)$: Net load TFM - Disturbance effect

$\mathbf{B}_{n\Gamma}$: Steady-state $\mathbf{B}(s)$ parameterized with Γ

$\mathbf{C}^c$: Decision variable for CVs selection

$\mathbf{C}_i$: Decision variable/Chromosome

$\mathbf{C}^m$: Decision variable for MVs selection

$\mathbf{C}^o$: Ad-hoc variable for control requisites

$\mathbf{C}^o_{f_{ij}}$: $\mathbf{C}^o$ for fault f_{ij}

$\mathbf{C}^r_{op}$: Optimal $\mathbf{C}^r$

$\mathbf{C}^p_i$: Real positive decision variable

$\mathbf{C}^q$: Decision variable for controller order selection

$\mathbf{C}^\Gamma$: Decision variable for controller interaction

$\mathbf{d}(s)$: Disturbance vector

$\mathbf{D}(s)$: Disturbance TFM

$\mathbf{D}_{fi}(s)$: $\mathbf{D}(s)$ without row i

$\mathbf{D}_r(s)$: Disturbance TFM for UVs

$\mathbf{D}_s(s)$: Disturbance TFM for CVs

f_{ij}: Fault in sensor i and actuator j

$\mathbf{F}(s)$: Diagonal low pass TFM filter

$\mathbf{G}(s)$: Process TFM

$\mathbf{G}_{ij(s)}$: $\mathbf{G}(s)$ without row i and column j

$\mathbf{G}_c(s)$: IMC controller TFM

$\mathbf{G}_r(s)$: Process TFM for UVs

$\mathbf{G}_s(s)$: Process TFM for CVs

$\tilde{\mathbf{G}}_s(s)$: Process model TFM for CVs

$\tilde{\mathbf{G}}_{s\Gamma}$: Steady-state matrix parameterized with Γ

m: Number of outputs

n: Number of inputs

n_g: Number of generations

n_i: Number of individuals

n_s: Number of individuals selected

NLE$_\Gamma$: Net load evaluation parameterized with Γ

p: Number of disturbances

p_c: Crossover probability

p_m: Mutation probability

$\mathbf{p}_i$: Vector with column permutation/Pairing

q: Number of control loops

q_a: Additional number of control loops

q_o: Ad-hoc number of control loops

s: Laplace variable

$\mathbf{S}_d(s)$: UVs TFM - Disturbance effect

$\mathbf{S}_{sp}(s)$: UVs TFM - Set point effect

SSD$_{\mathbf{a}}$: sum of square deviations of $\mathbf{a}$

t: Time

$\mathbf{T}^j_a$: Selection matrix for actuators

$\mathbf{T}^i_s$: Selection matrix for sensors

$\mathbf{u}(s)$: Input vector

$\mathbf{u}_{fj}(s)$: $\mathbf{u}(s)$ without entry j

$\mathbf{u}_r(s)$: Remaining inputs vector

$\mathbf{u}_s(s)$: MVs vector

v: Number of stabilizing control loops

$\mathbf{y}(s)$: Output vector

$\mathbf{y}_{fi}(s)$: $\mathbf{y}(s)$ without entry i

$\mathbf{y}_r(s)$: UVs vector

$\mathbf{y}_s(s)$: CVs vector

$\mathbf{y}_s^{net}(s)$: Net load effect TFM

$\mathbf{y}_s^{sp}(s)$: Set point vector

Greek

γ_{ij}: ij element of Γ

Γ: Parametrization binary matrix

Δ_i: Diagonal weighting matrix

Θ_i: Diagonal weighting matrix

Λ: RGA

λ_i: i-th eigenvalue

Λ_i: Diagonal weighting matrix

Λ_n: RGA number

Ξ_i: Diagonal weighting matrix

List of Algorithms

1 GA-based stochastic global search 29

List of Tables

1 SSD and NLE indexes used by the EMSD approach 29
2 TEP variables 30
3 GA parameter settings - Modified EMSD approach 30
4 Optimal solutions - Classical and modified EMSD approach 31
5 Sensor faults effect 31
6 PWC redesign - Sensor faults - TEP 31

List of Figures

1 Extended minimum square deviations (EMSD) approach 32
2 The SSD-NLE combined index approach 32
3 Tennessee Eastman process with stabilizing control loops. 33
4 IAEs main process variables - Optimal PWC structures 33
5 Dynamic performance - Optimal PWC structures 34
6 Modifications to the OPWC_{ff} for handling f_1, f_3, and f_5 34
7 Reactor Pressure (y_9) - PWC structures with and without redesign 35

Algorithm 1: GA-based stochastic global search

Initialization: $j = 0$, setting n_i, n_g, n_s, p_c, p_m, n_c, and $\mathbf{P}_j = [\mathbf{C}_1^T, \ldots, \mathbf{C}_{n_i}^T]_{n_i \times n_c}^T$;

while *($j \leq n_g$)* **do**

  Fitness evaluation: evaluate $f(\mathbf{C}_i^d)$ for each individual $\mathbf{C}_i^d$ from the current population set $\mathbf{P}_j$. The best individual is stored in the best population set $\mathbf{P}_b$ and its value in the vector $\mathbf{F}$;

  Selection: the n_s best individuals are selected using their relative fitness values and stored in $\mathbf{P}_s$. The $n_i - n_s$ remaining individuals are discarded;

  Recombination: the individuals in $\mathbf{P}_s$ are recombining by the crossover operator and stored in $\mathbf{P}_r$;

  Mutation: the recombined individuals in $\mathbf{P}_r$ suffer the mutation process and new genetic structures are obtained and stored in $\mathbf{P}_m$;

  Merging: $j = j + 1$ and both selected and mutated populations are merging together to give the next generation of individuals, $\mathbf{P}_j = [\mathbf{P}_s^T, \mathbf{P}_m^T]^T$;

end

Result: the best population set $\mathbf{P}_b$ $(j \times n_c)$ and the fitness profile $\mathbf{F}$ $(j \times 1)$

Table 1: SSD and NLE indexes used by the EMSD approach

Case	Index	Problem size
I	$\text{SSD}_{\mathbf{u}_s}(\mathbf{C}^m) = \|\|\mathbf{G}_s(\mathbf{C}^m)^{-1}\|\|_F^2 + \|\|\mathbf{G}_s(\mathbf{C}^m)^{-1}\mathbf{D}_s(\mathbf{C}^m)\|\|_F^2$	$n!/(q!(n-q)!)$
II	$\text{SSD}_{\mathbf{y}_r}(\mathbf{C}^c, \mathbf{C}^m) = \|\|\mathbf{S}_{sp}(\mathbf{C}^c, \mathbf{C}^m)\|\|_F^2 + \|\|\mathbf{S}_d(\mathbf{C}^c, \mathbf{C}^m)\|\|_F^2$	$[(m-q_o)!/(q_a!(m-q)!)][n!/(q!(n-q)!)]$
III	$\text{SSD}_{\mathbf{y}_r}(\mathbf{C}^c) = \|\|\mathbf{S}_{sp}(\mathbf{C}^c)\|\|_F^2 + \|\|\mathbf{S}_d(\mathbf{C}^c)\|\|_F^2$	$(m-q_o)!/(q_a!(m-q)!)$
All	$\text{NLE}_\Gamma = \|\|\mathbf{I} - \tilde{\mathbf{G}}_s(\Gamma)\mathbf{G}_s^{-1}\|\|_F^2 + \|\|\tilde{\mathbf{G}}_s(\Gamma)\mathbf{G}_s^{-1}\mathbf{D}_s\|\|_F^2$	$2^{(q \times q)}$

Table 2: TEP variables

no.	**Inputs**	**Variable**
u_1	D Flow [kg/h]	$XMV(1)$
u_2	A Flow [kg/h]	$XMV(3)$
u_3	A/C Flow [kscmh]	$XMV(4)$
u_4	Compressor rec. valve [%]	$XMV(5)$
u_5	Purge valve [%]	$XMV(6)$
u_6	Stripper steam valve [%]	$XMV(9)$
u_7	RCWO temp. setpoint [°C]	$XME(21)sp$
u_8	CCW Flow [m3/h]	$XMV(11)$
	Outputs	
y_1	Recycle flow [kscmh]	$XME(5)$
y_2	Reactor flow [kscmh]	$XME(6)$
y_3	Reactor temp. [°C]	$XME(9)$
y_4	Separator temp. [°C]	$XME(11)$
y_5	Separator pressure [kPa]	$XME(13)$
y_6	Stripper pressure [kPa]	$XME(16)$
y_7	Stripper temp. [°C]	$XME(18)$
y_8	Compressor work [kW]	$XME(20)$
$y_9(*)$	Reactor pressure [kPa]	$XME(7)$
$y_{10}(*)$	Production rate [m3/h]	$XME(17)$
$y_{11}(*)$	B comp. purge [mol%]	$XME(30)$
$y_{12}(*)$	G/H comp. ratio	$XME_{G/H}$
	Disturbances	
d_1	Composition stream 4 (A/C)	$IDV(1)$
d_2	Composition stream 4 (B)	$IDV(2)$

Table 3: GA parameter settings - Modified EMSD approach

n_i	n_g	p_c	p_m	n_c	n_q	Selection	Crossover
1000	60	0.7	$0.7/n_c$	17	1	roulette-wheel	double-point

Table 4: Optimal solutions - Classical and modified EMSD approach

PWC	$\mathbf{C}_{op}^{q}$	$\mathbf{C}_{op}^{c}$								$\mathbf{C}_{op}^{m}$								SSD+NLE
Name	q_a	y_1	y_2	y_3	y_4	y_5	y_6	y_7	y_8	u_1	u_2	u_3	u_4	u_5	u_6	u_7	u_8	Index
Classical EMSD																		
OPWC1	1	0	0	0	0	0	0	0	1	1	1	1	0	1	0	1	0	21.60
OPWC2	2	1	0	0	0	0	0	0	1	1	1	1	1	1	0	1	0	27.53
SSD-NLE combined index approach																		
OPWC3	2	0	1	0	0	0	0	1	0	1	1	1	0	1	0	1	1	19.76

Table 5: Sensor faults effect

Fault	CV	PWC	Disturbances					Set Points				SSD+NLE
no.		Name	d1	d2	d3	d4	d5	sp1	sp2	sp3	sp4	Index
f_1	y_2	FPWC_{f1}	SD	✓	✓	✓	✓	✓	✓	✓	SD	73.23
f_2	y_7	FPWC_{f2}	✓	✓	✓	✓	✓	✓	✓	✓	✓	20.23
f_3	y_9	FPWC_{f3}	SD	✓	✓	✓	✓	⊗	✓	✓	✓	31.04
f_4	y_{10}	FPWC_{f4}	✓	✓	✓	✓	✓	✓	⊗	✓	✓	17.69
f_5	y_{11}	FPWC_{f5}	✓	SD	✓	✓	✓	✓	✓	⊗	✓	89.05
f_6	y_{12}	FPWC_{f6}	✓	✓	✓	✓	✓	✓	✓	✓	⊗	23.36

Table 6: PWC redesign - Sensor faults - TEP

Fault	PWC	$\mathbf{C}_{op}^{q}$	$\mathbf{C}_{op}^{c}$								$\mathbf{C}_{fi}^{o}$				$\mathbf{C}_{op}^{m}$								SSD+NLE
no.	Name	(q_a)	y_1	y_2	y_3	y_4	y_5	y_6	y_7	y_8	y_9	y_{10}	y_{11}	y_{12}	u_1	u_2	u_3	u_4	u_5	u_6	u_7	u_8	Index
f_1	OPWC_{f1}	2	1	0	0	0	0	0	1	0	1	1	1	1	1	1	1	0	1	0	1	1	21.09
f_3	OPWC_{f3}	3	0	1	0	0	0	1	1	0	0	1	1	1	1	1	1	0	1	0	1	1	19.83
f_5	OPWC_{f5}	2	0	0	0	0	0	0	1	1	1	1	0	1	1	1	1	0	1	1	0	0	31.53

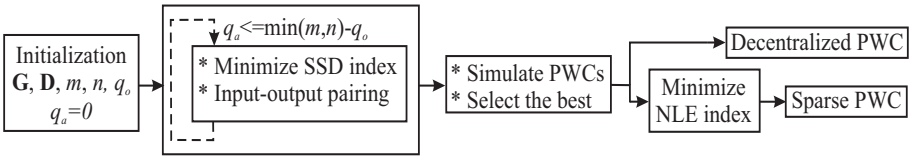

Figure 1: Extended minimum square deviations (EMSD) approach

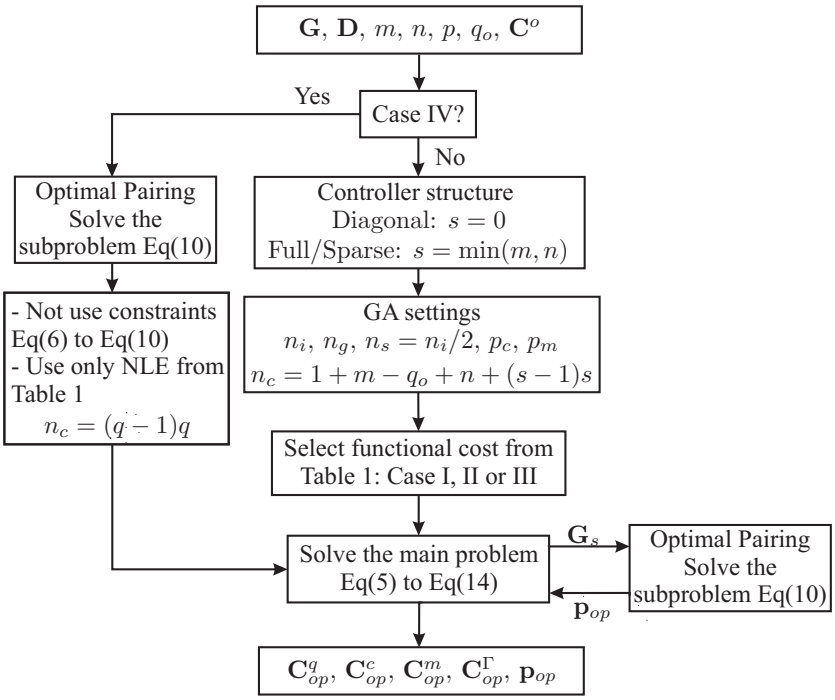

Figure 2: The SSD-NLE combined index approach

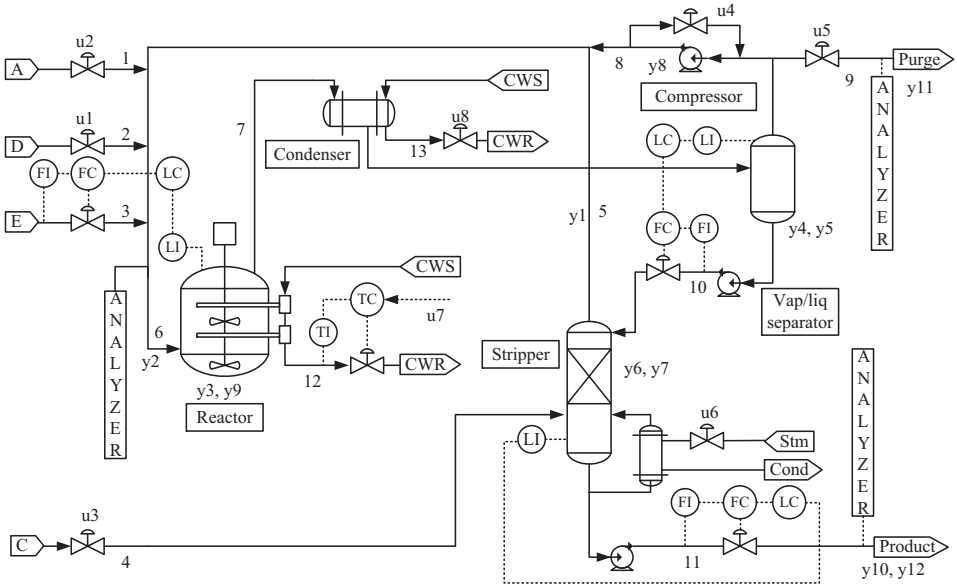

Figure 3: Tennessee Eastman process with stabilizing control loops.

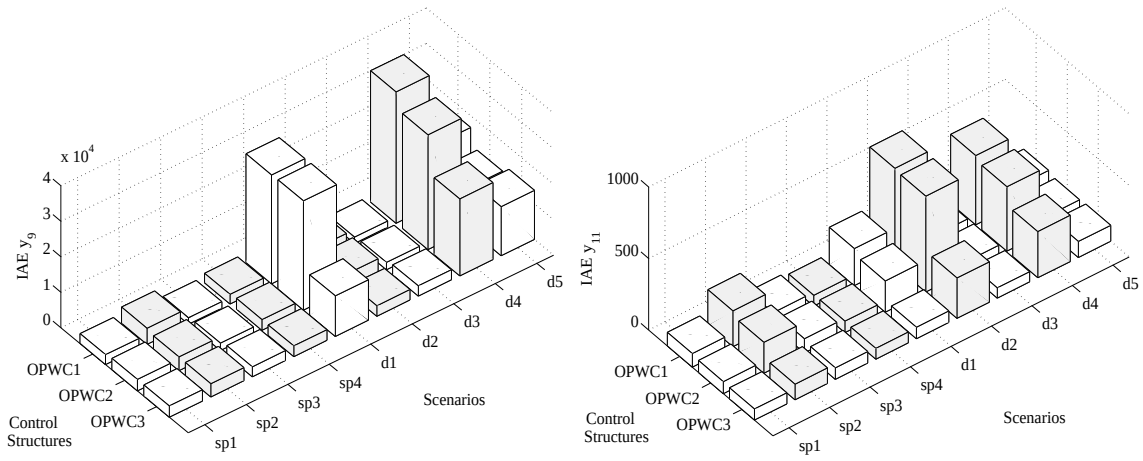

(a) Reactor pressure - y_9

(b) B comp. purge - y_{11}

Figure 4: IAEs main process variables - Optimal PWC structures

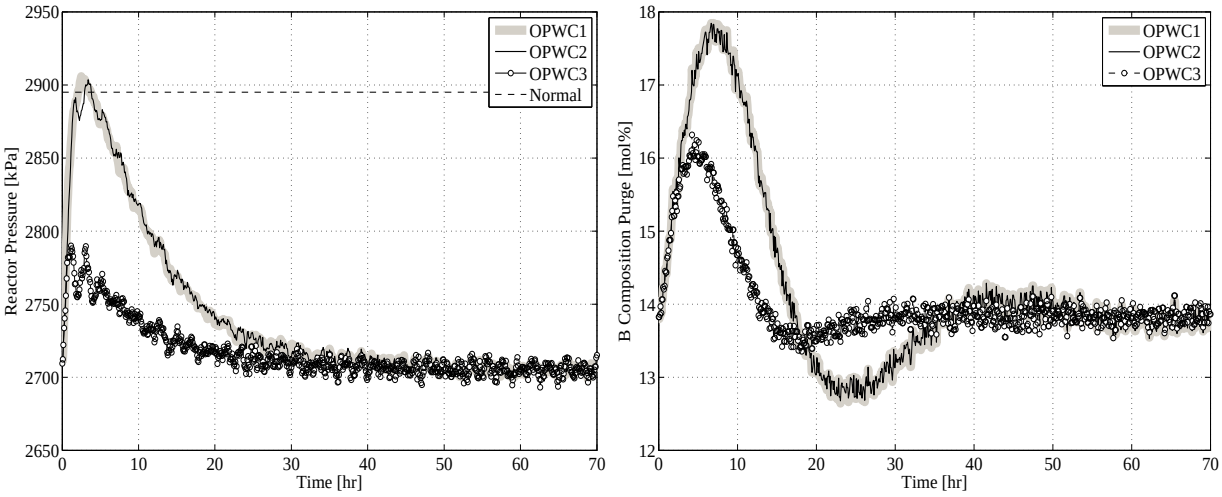

(a) Reactor pressure (y_9) - Scenario d1

(b) B composition purge (y_{11}) - Scenario d2

Figure 5: Dynamic performance - Optimal PWC structures

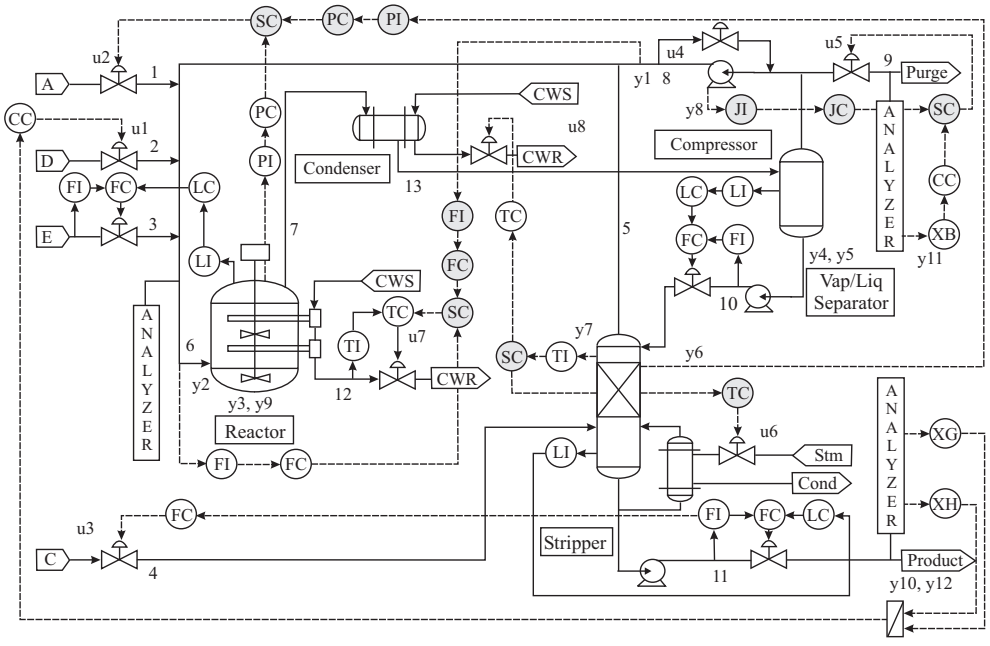

Figure 6: Modifications to the OPWC_{ff} for handling f_1, f_3, and f_5

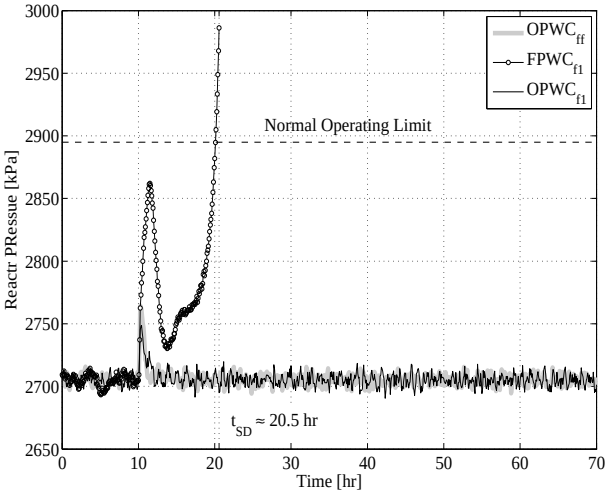

(a) Fault f_1 - Scenario sp4

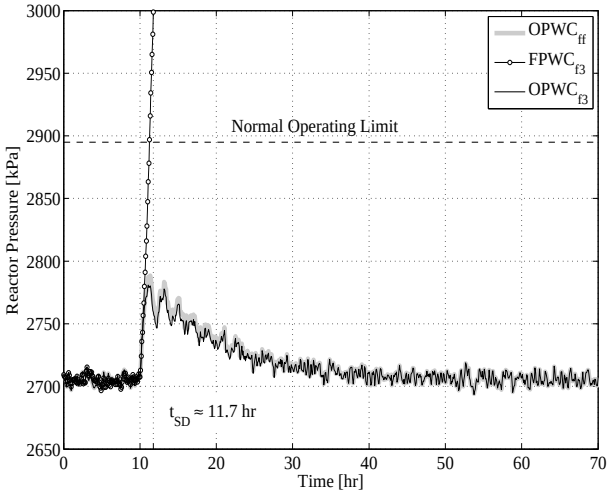

(b) Fault f_3 - Scenario d1

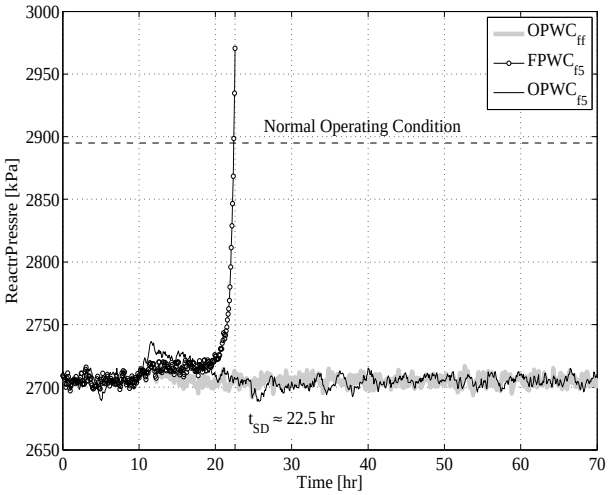

(c) Fault f_5 - Scenario d2

Figure 7: Reactor Pressure (y_9) - PWC structures with and without redesign